

Thermal explosion and runaway reaction simulation of lauroyl peroxide by DSC tests

Mei-Li You · Ming-Yang Liu · Sheng-Hung Wu · Jen-Hao Chi · Chi-Min Shu

Received: 27 March 2009 / Accepted: 16 April 2009 / Published online: 10 June 2009
© Akadémiai Kiadó, Budapest, Hungary 2009

Abstract Lauroyl peroxide (LPO) is a typical organic peroxide that has caused many thermal runaway reactions and explosions. Differential scanning calorimetry (DSC) was employed to determine the fundamental thermokinetic parameters that involved exothermic onset temperature (T_0), heat of decomposition (ΔH_d), and other safety parameters for loss prevention of runaway reactions and thermal explosions. Frequency factor (A) and activation energy (E_a) were calculated by Kissinger model, Ozawa equation, and thermal safety software (TSS) series via DSC experimental data. Liquid thermal explosion (LTE) by TSS was employed to simulate the thermal explosion development for various types of storage tank. In view of loss prevention, calorimetric application and model analysis to integrate thermal hazard development were necessary and useful for inherently safer design.

Keywords Activation energy (E_a) · Differential scanning calorimetry (DSC) · Exothermic onset temperature (T_0) · Heat of decomposition (ΔH_d) · Lauroyl peroxide (LPO) · Thermal safety software (TSS)

M.-L. You · S.-H. Wu · C.-M. Shu (✉)
Graduate School of Engineering Science and Technology,
National Yunlin University of Science and Technology, 123,
University Rd., Sec. 3, Douliou, Yunlin 64002, Taiwan, ROC
e-mail: shumc@yuntech.edu.tw

M.-L. You · M.-Y. Liu
Department of General Education, Chienkuo Technology
University, No. 1, Chieh Shou N. Rd., Changhua 50072, Taiwan,
ROC

J.-H. Chi
Department of Fire Science, Wu Feng Institute of Technology,
117, Chian-Kuo Rd., Sec. 2, Ming-Hsiung, Chiayi 62153,
Taiwan, ROC

Nomenclature

| | |
|------------|--|
| A | Frequency factor ($s^{-1} M^{1-n}$) |
| a | Vessel wetted surface area (m^2) |
| C_p | Liquid specific heat at constant pressure ($kJ kg^{-1} °C^{-1}$) |
| C_0 | Initial concentration (mole L^{-1}) |
| E_a | Activation energy ($kJ mol^{-1}$) |
| K | Pre-exponential factor (s^{-1}) |
| k_i | Rate at stage i (s^{-1}) |
| M | Mass of reactant (g) |
| m | Mass of reactor (kg) |
| n | Order of reaction (dimensionless) |
| P_{max} | Maximum pressure during overall reaction (psig) |
| \dot{Q} | Heat flow ($W g^{-1}$) |
| Q | Calorific capacity ($J g^{-1}$) |
| R | Ideal gas constant ($8.314 J mol^{-1} K^{-1}$) |
| S | Wetted surface area (m^2) |
| SADT | Self-accelerating decomposition temperature ($°C$) |
| T | Temperature ($°C$) |
| T_A | Final adjusted temperature (K) |
| T_{A0} | Initial adjusted temperature (K) |
| T_f | Final temperature ($°C$) |
| T_M | Final measured temperature (K) |
| T_0 | Exothermic onset temperature ($°C$) |
| T_{M0} | Initial measured temperature (K) |
| T_{NR} | Temperature of no return ($°C$) |
| T_{max} | Maximum temperature during overall reaction ($°C$) |
| T_{wall} | Temperature on the wall ($°C$) |
| TMR_{ad} | Time to maximum rate under adiabatic system (min, h) |
| U | Heat transfer coefficient ($kJ min^{-1} m^{-2} K^{-1}$) |
| ϕ | Thermal inertia (dimensionless) |

| | |
|------------------|--|
| $(dT/dt)^{-1}$ | Self-heating rate ($^{\circ}\text{C min}^{-1}$) |
| $(dT/dt)^{-1}_A$ | Actual self-heating rate ($^{\circ}\text{C min}^{-1}$) |
| α | Degree of conversion (dimensionless) |
| β | Heating rate ($^{\circ}\text{C min}^{-1}$) |
| ΔH_d | Heat of decomposition (J kg^{-1}) |
| λ | Heat conductivity (J ms K^{-1}) |

Introduction

Organic peroxides (OPs) when exothermically decomposed require inherently safer design during preparation, manufacturing, transportation, storage, and even disposal. They can release large amounts of thermal energy and result in enormous pressure during runaway excursion, leading to a fire or explosion accident [1, 2].

Lauroyl peroxide (LPO), which was produced commercially in 1941, is a white solid with a faint soapy odor, less dense than, and insoluble in, water. Hence, it floats on water. LPO is applied principally in the production of polymers [3, 4]. It is a strong free radical source containing more than 4.0 mass% of active oxygen, and is applied as a polymerization initiator or as a polymerization catalyst [5].

LPO is applied as bleaching agent, drying agent for fats, oils, and waxes, as a catalyst and vulcanizing agent. Thus, small amounts are employed in food packaging. It is an oxidizing agent, and it can ignite organic materials; hence it has dangerous fire and explosion risk. Strongly reduced materials, such as sulfides, nitrides, and hydrides may react explosively [6, 7]. It decomposes rapidly, causing fire and explosion hazard, on heating and under influence of light. It should be stored in a dry and refrigerated ($<27^{\circ}\text{C}$ recommended or 38°C max) area and be kept away from reducing agents and incompatible substances.

Differential scanning calorimetry (DSC) was employed to determine the fundamental reaction hazard of 95 mass% LPO. In parallel, the kinetic analysis method of Kissinger equation and Ozawa equation was applied to calculate the activation energy (E_a) and frequency factor (A) [8–10]. Finally, the thermal safety software (TSS) series applied to simulate a situation for thermal explosion under various vessel types.

Experimental design and methods

Sample

Ninety-five mass% LPO was directly purchased from the Fluka Co., and both density and concentration were measured. Then, LPO was stored in a refrigerator at 4°C .

Differential scanning calorimetry (DSC)

Dynamic scanning experiments were performed on a Mettler TA8000 system coupled with a DSC 821^e measuring test crucible (Mettler ME–26732) that could withstand relatively high pressure about 100 bar. STAR^e software was employed for acquiring thermal curves. For the sake of better thermal equilibrium, a heating rate (β) was chosen, such as $4^{\circ}\text{C min}^{-1}$. About 1–10 mg of the sample was selected for acquiring the experimental data. The test cell was sealed manually by a special tool equipped with Mettler's DSC, and we conducted dynamic scanning by starting the programmed setting.

DSC is regarded as a useful tool for evaluating thermal hazards and investigating decomposition mechanisms of reactive chemicals [11–13], if the experiments are carried out carefully. The experimental conditions were as follows:

- (1) Heating rate: 1, 2, 4, $10^{\circ}\text{C min}^{-1}$.
- (2) Materials mass: 1–10 mg.
- (3) Temperature range: $30\text{--}200^{\circ}\text{C}$.
- (4) Test cell: These gold-plated high-pressure crucibles, which can be pressed together, have proven to be very useful for safety investigation, but they can only be used for one measurement with a maximum pressure of 15 MPa. The lid is pressed into the crucible with a pressure of about a ton, therefore the seal tightens the crucible. A toggle press is used to close the crucible.

Thermal safety software (TSS)

The TSS includes three groups of the program that correspond to a three-stage approach [14, 15]. We fully exploited the liquid thermal explosion (LTE) model of Convex Fork on the TSS to simulate thermal explosion on a barrel. Here, CE-FK provided numerical simulation of thermal explosion development. These simulative data were necessary for proper choice of safe conditions in application, such as storage and transportation, specifically for an energetic chemical.

Thermal decomposition kinetics

The reaction mechanism of CHP could be represented by the following kinetic model:

Initiation reaction:



$$r_1 = k_0 \exp\left(-\frac{E_1}{RT}\right)(1 - \alpha)^n \quad (2)$$

Based upon the experimental data, the thermokinetic parameters, as listed in Table 1, could be applied to

simulate the thermal explosions under running with the software ConvEx Fork (CE-FK) on the TSS from CISP.

Thermal explosion simulation

The simulation project in CE-FK consists of three main parts [15]:

- (1) The configuration and dimension of a vessel, physical properties of a reacting liquid and material of the vessel's shell, and initial temperatures of shell and liquid.
- (2) Boundary conditions that define the type of heat exchange between the vessel and the environment.
- (3) Reaction kinetics.

Various vessel types were chosen for simulation, as such a tank is suitable for use in practice. CE-FK allows specifying boundary conditions of the first, second, and third type. They are assumed to be uniform over each reactor surface and can be specified for each surface, separately.

Boundary conditions of the first type (1st):

$$T_{\text{wall}} = g_1(t) \quad (3)$$

Here, $g_1(t)$ denotes a function that gives the time dependence of temperature on the wall.

Boundary conditions of the second type (2nd):

$$q_{\text{wall}} = -\lambda \frac{\partial T}{\partial r_{\text{wall}}} = g_2(t) \quad (4)$$

Here $g_2(t)$ represents a function that gives the time dependence of heat flux on the wall.

Boundary conditions of the third type (3rd):

$$q_{\text{wall}} = -\lambda \frac{\partial T}{\partial r_{\text{wall}}} = g_1(t)(T_{\text{wall}} - g_2(t)) \quad (5)$$

Here $g_1(t)$ and $g_2(t)$ are functions that give the time dependence of the heat transfer coefficient and of the ambient temperature.

This study simulated various conditions for the barrel, such as normal storage at 37 °C (No. 1 test), runaway reaction temperature condition at 60 °C (No. 2 test), early step of external fire circumstance at 120 °C (No. 3 test) and fire conditions at 250 °C (No. 3 test). At storage, the ambient temperature will be equal to room temperature (30–37 °C for summer); the heat transfer coefficient (HTC) for a barrel staying outdoors without wind was about 10 W m² K⁻¹. If we were to analyze accidental fire

conditions, the ambient temperature would be much higher than the cooling failure and the HTC might also be higher, because, in this case, air is moved around the barrel. We took a temperature of about 250–300 °C and HTC of about 20 W m² K⁻¹ to simulate the fire condition. The boundary conditions are given in Table 2.

This study divided the barrel into three surfaces: top, side, and bottom. The boundary conditions on the side and top surfaces were assumed to be the 3rd type. In practice, the barrel is built on the ground; therefore, the bottom is in close contact with the ground. Accordingly, it was reasonable to define conditions of the 1st type and take its temperature equal to the ambient one.

It should be noted that the simulation was carried out by assuming that the influence of the shell can be neglected. The kinetic model created on the basis of the DSC data completes the project. The model (the kinetic parameters are listed in Table 1) was imported from the ForK data base.

Results and discussion

Fundamental reaction hazard determination

To evaluate the thermal hazard of 95 mass% LPO, DSC under various scanning rates was applied to determine thermokinetics, as illustrated in Fig. 1. Figure 1 demonstrates a comparison of thermal curves of decomposition of 95 mass% LPO with four types of β ($\beta = 1, 2, 4,$ and $10 \text{ }^\circ\text{C min}^{-1}$) by DSC. The initial reaction of LPO was endothermic when temperature exceeded 40 °C that caused a phase change at the moment. When β value was lower, the decomposition reaction could be detected at a lower temperature. On the other hand, if β value was higher, the T_0 determined could delay decomposition and the maximum of temperature (T_{max}) was correspondingly higher.

According to Fig. 1, LPO decomposed at 60 °C. Table 3 displays thermokinetics data and safety parameters of 95 mass% LPO by STAR^c program of DSC. T_0 of LPO was about 60–70 °C. In accordance with the experimental results, the reaction model was identified as an n-order reaction. E_a was estimated at 100 kJ mol⁻¹ by STAR^c program of DSC. As a result, a rapid temperature increase of LPO may cause a dramatic decomposition reaction under external fire conditions. According to Fig. 1, LPO produced a great deal of heat. The ΔH_d for LPO was about 500–600 J g⁻¹ under various heating rates by DSC.

Kinetic analysis

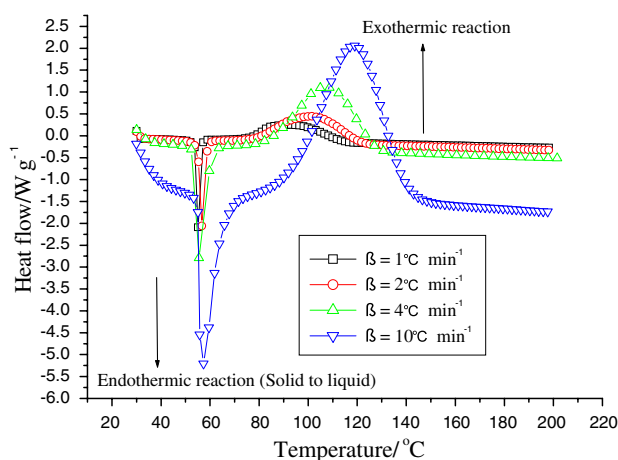
The kinetic analysis of the step was done by various heating rate methods based on the equations of Kissinger

Table 1 Simulation of calorific capacity and apparent activation energy

| K_1 (s ⁻¹) | n | Q (kJ kg ⁻¹) | E_a (kJ mol ⁻¹) |
|--------------------------|---|--------------------------|-------------------------------|
| 26 | 1 | 600 | 90 |

Table 2 The boundary parameter of CE-FK by various scenarios

| | No. 1 Top (°C) | No. 1 Side (°C) | No. 1 Bottom (°C) | No. 2 Top (°C) | No. 2 Side (°C) | No. 2 Bottom (°C) | No. 3 Top (°C) | No. 3 Side (°C) | No. 3 Bottom (°C) |
|--|-------------------|--------------------|----------------------|-------------------|--------------------|----------------------|-------------------|--------------------|----------------------|
| Ambient temperature (°C) | 37 | 37 | 20 | 60 | 60 | 20 | 120 | 120 | 20 |
| HTC/W (m ² K) ⁻¹ | 10 | 10 | 0 | 10 | 10 | 0 | 20 | 20 | 0 |
| Boundary condition type | 3rd | 3rd | 1st | 3rd | 3rd | 1st | 3rd | 3rd | 1st |

**Fig. 1** Heat flow versus temperature of LPO under various heating rates by DSC

and Ozawa. The T_{max} and equation parameters for reaction from DSC analysis were given in Table 4. The Kissinger and Ozawa methods are based on various heating rates which depend on the T_{max} in DSC. The kinetic analysis methods were as follows:

Kissinger method [16]:

$$\frac{2.303d[\log(\beta/T_{max}^2)]}{d(1/T_{max})} = -E_a/R \quad (6)$$

where T_{max} is the temperature corresponding to the maximum in the DSC exothermic at a heating rate (β). From the slope of the linear plot of $\log(\beta/T_{max}^2)$ against T_{max}^{-1} , E_a can be calculated.

Ozawa method [17–19]:

$$\frac{2.15d[\log(\beta)]}{d(1/T_{max})} = -E_a/R \quad (7)$$

Table 3 Safety parameters of LPO under various heating rates by DSC tests

| β (°C min ⁻¹) | m (mg) | $T_{endo.}$ (°C) | $\Delta H_{endo.}$ (J g ⁻¹) | T_0 (°C) | ΔH_d (J g ⁻¹) | T_{max} (°C) |
|---------------------------------|--------|------------------|---|------------|-----------------------------------|----------------|
| 1 | 5.0 | 40 | -145 | 60 | 632 | 92 |
| 2 | 8.0 | 40 | -150 | 65 | 625 | 101 |
| 4 | 6.0 | 42 | -170 | 70 | 576 | 107 |
| 10 | 9.0 | 45 | -197 | 75 | 518 | 118 |

where E_a was obtained from the slope of the plot of $\log \beta$ against T_{max}^{-1} .

Table 4 was used to calculate the E_a and A. The results show the E_a of Kissinger method that was about 91 kJ mol⁻¹ as shown in Table 5. Another method was determined to be about 90 kJ mol⁻¹ of E_a as shown in Figs. 2 and 3.

Thermal explosion simulation of LPO

This study simulated four temperature situations: 37 °C (normal condition), 60 °C (runaway reaction temperature), 120 °C (early step for external fire situation) and 250 °C (fire circumstance) of 95 mass% LPO stored in various storage tanks that included A1 (height = 1 m and radius = 0.5 m), A2 (height = 2 m and radius = 1 m) and A3 (height = 4 m and radius = 2 m). In normal condition, the ambient temperature equals room temperature (30–37 °C in summer season in Taiwan) and the heat transfer coefficient (HTC) for a barrel staying outdoors with no wind was about 10 W (m² K)⁻¹. If we were to analyze accidental fire exposure, the ambient temperature would be much higher than cooling failure and the HTC might also be higher, because in this case, air moves around the drum. We took a temperature of 250–300 °C for the fire exposure condition, and HTC could be taken at about 20 W (m² K)⁻¹.

From simulated results, the normal condition without wind effect, the T_{max} in the tank was simulated to exceed 200 °C (software setup ourselves), as displayed in Fig. 4. All of the tests calculated the limit of T_{max} that was set at 200 °C by ourselves, because of the emergency response time being exceeded.

Figures 4, 5, 6, and 7 disclose the temperature versus time curves for the thermal decomposition simulation on various storage types under differential conditions. After many tests and runs, the critical temperature (T_c) of the

Table 4 The calculation of E_a and A in this study

| β ($^{\circ}\text{C min}^{-1}$) | T_{max} ($^{\circ}\text{C}$) | $(T_{\text{max}} \times 10^3)^{-1}$ ($^{\circ}\text{C}$) | $\log(\beta \times T_{\text{max}}^{-2})/\text{Kissinger method}$ | $\log(\beta)/\text{Ozawa method}$ |
|---|---|--|--|-----------------------------------|
| 1 | 91.2 | 2.75 | -11.80 | 0.00 |
| 2 | 101.4 | 2.67 | -11.16 | 0.65 |
| 4 | 108.4 | 2.62 | -10.50 | 1.29 |
| 10 | 118.0 | 2.55 | -9.63 | 2.15 |

Table 5 The calculation of E_a and A in this study with different methods in this study

| Analysis method | E_a (kJ mol^{-1}) | A (s^{-1}) | n |
|-----------------|--------------------------------|-------------------------|-----|
| DSC | 100 | 2.0×10^{11} | 1 |
| Kinssger method | 91 | 7.1×10^{10} | NA |
| Ozawa method | 90 | 8.1×10^{12} | NA |
| TSS | 90 | 8.1×10^{12} | 1.2 |

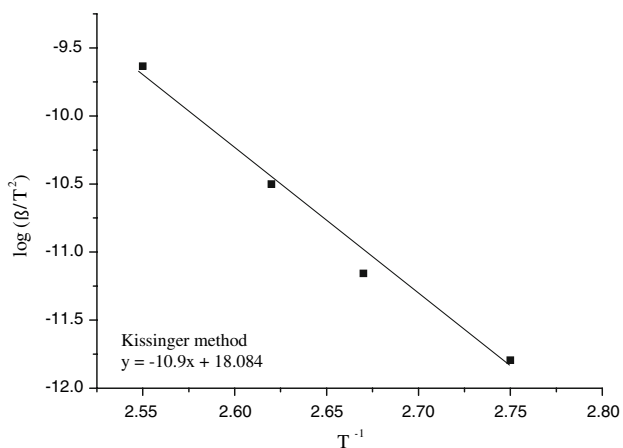


Fig. 2 Heat flow versus temperature of 98 mass% LPO comparing with H_2O and fire-extinguishing chemical under heating rates at $4\text{ }^{\circ}\text{C min}^{-1}$ by DSC

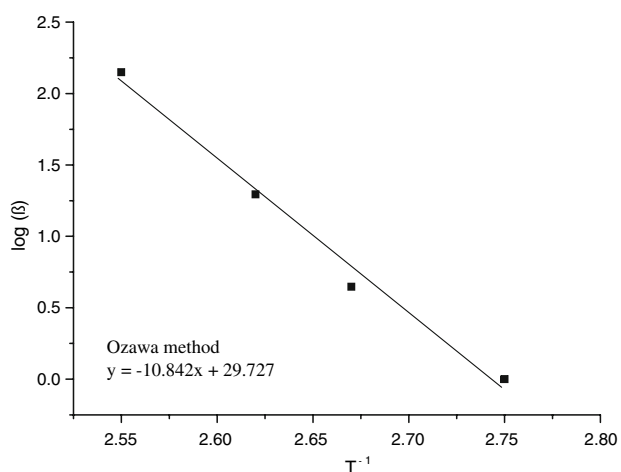


Fig. 3 Heat flow versus temperature of 95 mass% LPO comparing with H_2O and fire-extinguishing chemical under heating rates at $4\text{ }^{\circ}\text{C min}^{-1}$ by DSC

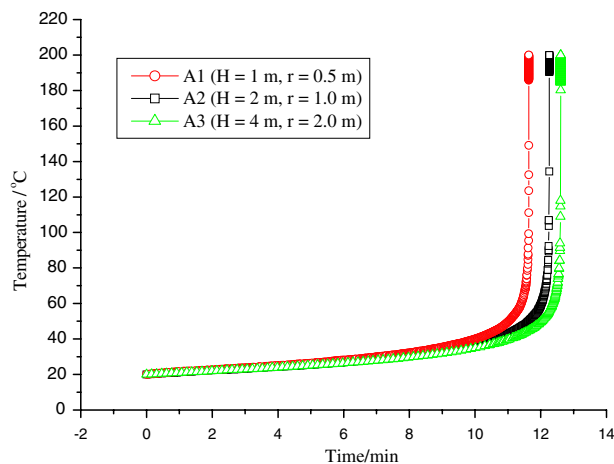


Fig. 4 Temperature versus time for thermal explosion simulation by CE-FK under room temperature ($37\text{ }^{\circ}\text{C}$) situation with various storage vessel sizes

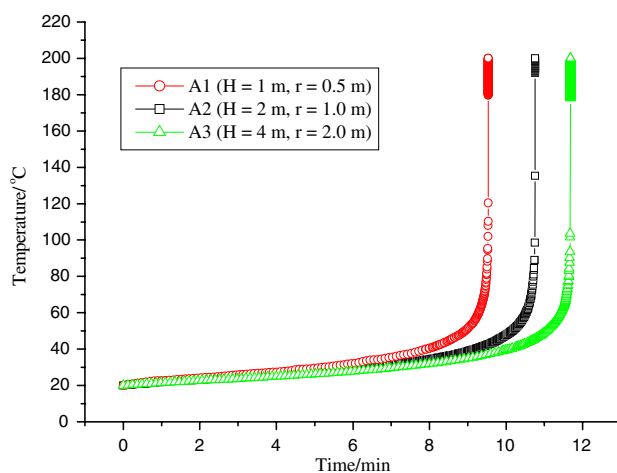


Fig. 5 Temperature versus time for thermal explosion simulation by CE-FK under runaway reaction temperature ($60\text{ }^{\circ}\text{C}$) with various storage vessel sizes

normal condition and fire conditions was about 45 and 35 $^{\circ}\text{C}$, respectively. Safety index, such as self-accelerating decomposition temperature (SADT), T_c , temperature of no return (T_{NR}), time to maximum rate (TMR), etc., was broadly used to keep the safe handling environment. Table 6 is a useful tool that was used to note the emergency response time on TMR.

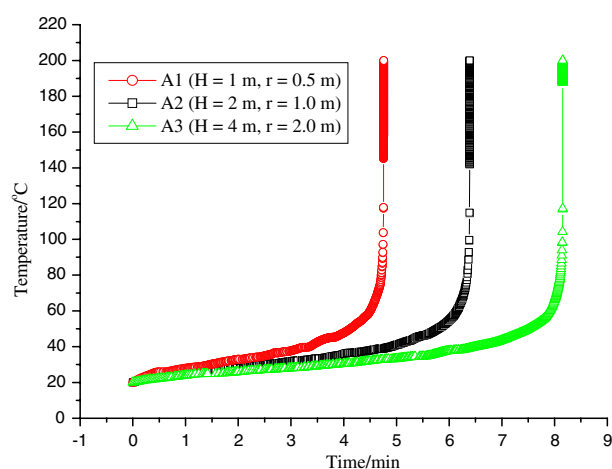


Fig. 6 Temperature versus time for thermal explosion simulation by CE-FK under early step of external fire exposure situation (120 °C) with various storage vessel sizes

Table 6 A useful tool to note the emergency response time on TMR in this study

| Vessel type | TMR under 37 °C/min | TMR under 60 °C/min | TMR under 120 °C/min | TMR under 250 °C/min |
|----------------|---------------------|---------------------|----------------------|----------------------|
| H = 1, r = 0.5 | 11.6 | 9 | 4.7 | 2.7 |
| H = 2, r = 1 | 12.2 | 11 | 6.3 | 4.0 |
| H = 4, r = 2 | 12.6 | 12 | 8.1 | 5.6 |

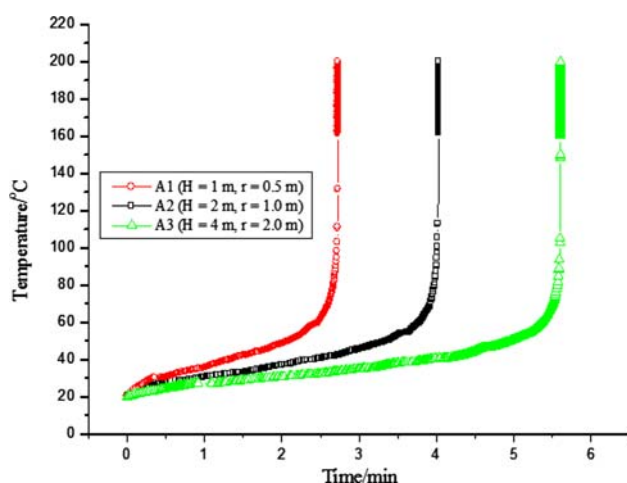


Fig. 7 Temperature versus time for thermal explosion simulation by CE-FK under external fire exposure situation (250 °C) with various storage vessel sizes

Conclusions

LPO possesses a high reaction rate substance of OPs. Thermal explosion development of LPO was analyzed at a temperature at 50 °C that exceeds phase changing in a storage tank. TMR of LPO is the emergency response time that was analyzed in

Table 6. According to thermal explosion simulation curves analysis, all of thermal explosion initiation of LPO started at 50 °C. LPO must be stored in a cooling storage environment and must avoid any sunlight illumination.

Acknowledgements The authors are indebted to the donors of the National Science Council (NSC) in Taiwan under the contract No. NSC-96-2625-Z-224-001 for financial support. The authors would also like to thank Dr. Kuo-Ming Luo for valuable suggestions on experiments and the measurements of a runaway reaction.

References

1. Wu SH, Wang YW, Wu TC, Hu WN, Shu CM. Evaluation of thermal hazards for dicumyl peroxide by DSC and VSP2. *J Therm Anal Calorim.* 2008;93(1):189–94.
2. Chen JR, Wu SH, Lin SY, Hou HY, Shu CM. Utilization of microcalorimetry for an assessment of the potential for a runaway decomposition of cumene hydroperoxide at low temperatures. *J Therm Anal Calorim.* 2008;93(1):127–33.
3. Tournier L, Zard SZ. A direct approach to α -hydroxy and α -chloro trifluoromethyl derivatives. *Tetrahedron Lett.* 2005;46:455–9.
4. Yang D, Koseki H, Hasegawa K. Predicting the self-accelerating decomposition temperature (SADT) of organic peroxides based on non-isothermal decomposition behavior. *J Loss Prev Process Ind.* 2003;16(5):411–6.
5. Bevington JC, Hunt BJ. The use of stabilized radicals with monomers and lauroyl peroxide. *Eur Polym J.* 2004;40(1):103–8.
6. Material Safety Data Sheet (MSDS) for LPO, Industrial Technical Research Institute, Hsinchu, Taiwan, ROC;2006.
7. Guidelines for Chemical Reactivity Evaluation and Application to Process Design, CCPS. AICHE. New York, USA; 1995.
8. Belichmeier JA, Cammenga HK, Schneider PB, Steer AG. A simple method for determining activation energies of organic reactions from DSC curves. *Thermochim Acta.* 1998;310:147–51.
9. Tseng JM, Chang YY, Su TS, Shu CM. Study of thermal decomposition of methyl ethyl ketone peroxide using DSC and simulation. *J Hazard Mater.* 2007;142:765–70.
10. Wu KW, Hou HY, Shu CM. Thermal phenomena studies for dicumyl peroxide at various concentrations by DSC. *J Therm Anal Calorim.* 2006;83:41–4.
11. Ando T, Fujimoto T, Morisaki S. Analysis of differential scanning calorimetric data for reactive chemical. *J Hazard Mater.* 1991;28:251–80.
12. Maria G, Heinzle E. Kinetic system identification by using shortcut techniques in early safety assessment of chemical processes. *J Loss Prev Process Ind.* 1998;11:187–206.
13. STARe Software with Solaris Operating System, Operating Instructions, Mettler Toledo, Switzerland; 2004.
14. Thermal Safety Software (TSS), ChemInform Saint Petersburg Ltd. (CISP); 2009.
15. Chen KY, Wu SH, Wang YW, Shu CM. Runaway reaction and thermal hazards simulation of cumene hydroperoxide by DSC. *J Loss Prev Process Ind.* 2008;21:101–9.
16. Kissinger HE. Variation of peak temperature with heating rate in differential thermal analysis. *J Res Natl Bur Stand.* 1956;57:217–21.
17. Ozawa T. Kinetic analysis of derivative curves in thermal analysis. *J Therm Anal.* 1970;2:301–24.
18. Ozawa T. Critical investigation of methods for kinetic analysis of thermoanalytical data. *J Therm Anal.* 1975;7:601–17.
19. Ozawa T. A modified method for kinetic analysis of thermoanalytical data. *J Therm Anal.* 1976;9:369–73.